

Conformational transformations induced by the charge-curvature interaction: Mean-field approach

Yu. B. Gaididei

Bogolyubov Institute for Theoretical Physics, Metrologichna Street 14 B, 01413, Kiev, Ukraine

P. L. Christiansen

Informatics and Mathematical Modeling and Department of Physics, The Technical University of Denmark, DK-2800 Lyngby, Denmark

W. J. Zakrzewski

Department of Mathematical Sciences, University of Durham, Science Laboratories, South Road, Durham DH1 3LE, England

(Received 21 March 2005; published 16 August 2006)

A simple phenomenological model for describing the conformational dynamics of biological macromolecules via the nonlinearity-induced instabilities is proposed. It is shown that the interaction between charges and bending degrees of freedom of closed molecular aggregates may act as drivers giving impetus to conformational dynamics of biopolymers. It is demonstrated that initially circular aggregates may undergo transformation to polygonal shapes and possible application to aggregates of bacteriochlorophyll *a* molecules is considered.

DOI: [10.1103/PhysRevE.74.021914](https://doi.org/10.1103/PhysRevE.74.021914)

PACS number(s): 87.15.-v, 63.20.Pw, 63.20.Ry

I. INTRODUCTION

The functioning of biological macromolecules is determined by their tertiary structure and different types of semiflexible polymers in solutions exhibit a variety of conformational phase transitions [1]. Even modest conformational changes modify long-range electronic interactions in oligopeptides [2], they may remove steric hindrances and open the pathways for molecular motions which are not available in rigid proteins [3]. In particular, it has been recently shown [4] that flexibility increases the hydrogen accessibility of DNA fragments and in this way facilitates strand breaks in DNA molecules.

The electronic conduction properties of DNA have recently attracted much attention because of their relevance in such biologically important processes as damage, mutation, and repair of DNA [5–7]. Experiments [8] and *ab initio* calculations [9] provide some evidence that DNA may be considered as a semiconductor where electrons (or holes) added to an otherwise empty band (conduction band for electrons and filled valence band for holes) are strongly coupled with vibrational modes and the conduction is due to the thermal motion of small polarons [10–12]. The conduction of poly(dA)-poly(dT) is due to negatively charged polarons while positively charged polarons are in poly(dG)-poly(dC) [8]. Calculations of DNA molecular dynamics have showed that nonlinear mechanisms might lead to the existence of “vibrational hot spots,” where the trapping of charge can occur [12].

In the main part of the previous studies of the electronic properties of DNA the charge-lattice coupling included compression and torsion of the base pairs as well as internal motion of the base pair molecules. Research in solitonic properties of the chains with a bending has been initiated in recent years [13–17]. In particular, it was shown that the bending of the chain could manifest itself as an effective trap

for nonlinear excitations [13,15,17] and that the energy of excitations decreases when the curvature of the bending increases [15]. A phenomenological model for describing the conformational dynamics of biopolymers via the nonlinearity-induced buckling and collapse instability was proposed in Ref. [18]. Buckling instability of semiflexible polyelectrolytes with intrachain attractions due to counterion correlations was studied in Ref. [19].

Recent DNA cyclization experiments [20], which have shown the facile *in vitro* formation of DNA circles shorter than 30 nm (100 base pairs), opened a new exciting area of research where an interaction of charge carriers with bending degrees of freedom of *closed* molecular chain is crucial.

The geometric structure of bacterial light-harvesting (LH) complexes, supramolecular machines which transform the solar energy into a charge separation, is also flexible and plays an important role in the photosynthesis [21]. The x-ray crystallography shows [22] that bacteriochlorophyll *a* (Bchl-*a*) molecules in the LH complex are organized into two concentric rings: the B800 and B850 rings. The former consists of nine well-separated Bchl-*a* molecules with an absorption band at 800 nm and the latter consists of 18 Bchl molecules with an absorption band at 860 nm (see Fig. 1 in Ref. [23]). Based on single-molecule fluorescence spectroscopy experiments, it has been shown that the shape of the LH2 complexes can deviate from the ideally circular shape of the complex in crystals [23–26]. Recently an oblate plate shape of the LH2 complex from bacteria *Rhodobacter spheroides* 2.4.1 in detergent solution has been determined from synchrotron small-angle x-ray scattering data [27]. Based on atomic force microscopy experiments which showed a variety of shapes and conformations for light-harvesting LH1 complexes and different types of their packing in two-dimensional crystals, it has been proposed that the rich and flexible geometric structure of light harvesting complexes arises from the H-bonding patterns that stabilize binding of

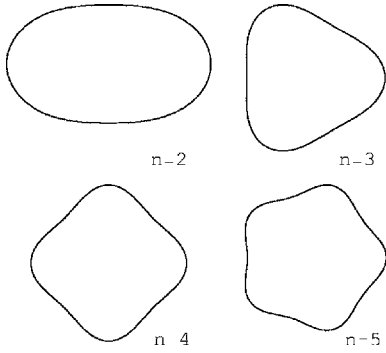


FIG. 1. The shape of the chain: in the ellipselike state ($n=2$), in the polygon states ($n=3,4,5$).

the Bchl's to the light harvesting polypeptides [28]. It is well known that hydrogen bonded systems (such as hydrogen bonded water molecules) are often excellent proton conductors (see, e.g., Ref. [29]). The charge transport in these systems is due to coupled motion of ionic and orientational defects [30]. It is of interest and importance, therefore, to study the role of mobile defects in the shaping of the light harvesting complexes.

The main aim of this paper is to develop a simple, generic model for electron-curvature interactions on closed molecular aggregates. In what follows we will be mostly concerned with the role of electrons (holes) in closed DNA-like semiflexible polymers. Our approach to the conformational properties of light-harvesting complexes which we present in Sec. VI, is based on the suggestion that the flexible geometry of LH complexes is due to mobile charges carriers in the hydrogen-bonded networks. We show that the presence of charge modifies (softens or hardens) the local chain stiffness. We consider the mean field theory, where the thermal fluctuations are ignored; we find that due to the interaction between electrons and the bending degrees of freedom the circular shape of the aggregate may become unstable and the aggregate takes the shape of an ellipse or, in general, of a polygon. The shape instability is associated with nontrivial periodic solutions of the nonlinear Schrödinger equation. We determine how ν_n , the critical charge density at which transformation to an n -gon shape occurs, depends on the parameters of the system (electron hopping integral, chain stiffness and strength of the electron-curvature coupling). Below this value the shape of aggregate is circular whereas above the instability point, the aggregate takes a polygon shape. The role of interaggregate interaction is also investigated. It is shown that the interaction between aggregates may stabilize the ringlike shape. The paper is organized as follows. In Sec. II we describe a model. In Sec. III we present an analytical solution to the Euler-Lagrange equation. In Sec. IV we compare our analytical results to results obtained directly by numerical simulations. In Sec. V the interplay between shape of complexes and intercomplex interaction is studied. Section VI is devoted to application to conformational transformations in light-harvesting complexes. Section VII presents some concluding remarks.

II. THE MODEL

Let us consider a polymer chain consisting of L units (for DNA each unit is a base pair) labeled by an index l , and

located at the points $\vec{r}_l = \{x_l, y_l, z_l\}$ ($l=1, \dots, L$). We are interested in the case when the chain is closed and so we impose the periodicity condition on the coordinates \vec{r}_l

$$\vec{r}_l = \vec{r}_{l+L}. \quad (1)$$

To describe the chain flexibility we use a discrete wormlike chain model. In the frame of this model the chain flexibility is accounted for by employing a microstructure consisting of many sequentially joined rods which connect base pairs and by incorporating a bend potential at each point of rotation [31]. Thus the bending energy of the chain has the form

$$U_b = \frac{k}{2} \sum_l \frac{\kappa_l^2}{1 - \kappa_l^2 / \kappa_{\max}^2}, \quad (2)$$

where

$$\kappa_l \equiv \frac{1}{a} |\vec{r}_{l+1} + \vec{r}_{l-1} - 2\vec{r}_l| = 2 \sin \frac{\alpha_l}{2} \quad (3)$$

determines the curvature of the chain at the point l . Here α_l is the angle between the tangent vectors $\vec{r}_{l+1} - \vec{r}_l$ and $\vec{r}_l - \vec{r}_{l-1}$, a is an equilibrium distance between units (in what follows we assume $a=1$), k is the elastic modulus of the bending rigidity (spring constant) of the chain. Note that to avoid too large bending deformations we have introduced the term $\kappa_l^2 / \kappa_{\max}^2$ in the denominator of Eq. (2). Here the parameter $\kappa_{\max} = 2 \sin(\alpha_{\max}/2)$ is the maximum local curvature with α_{\max} being the maximum bending angle.

In addition to the bending angle, there is a degree of freedom at each segment l , $l+1$ describing the change of the distance $|\vec{r}_l - \vec{r}_{l+1}|$ between units. We take the corresponding stretching energy in the form

$$U_s = \frac{\sigma}{2} \sum_l (|\vec{r}_l - \vec{r}_{l+1}| - a)^2, \quad (4)$$

where σ is an elastic modulus of the stretching rigidity of the chain.

We assume that there is a small amount of mobile carriers (electrons, holes in the case of DNA, protons in the case of hydrogen bonded systems) on the chain. We take the simplest theoretical model for the carriers, a nearest-neighbor tight binding Hamiltonian of the form

$$H_{el} = E_0 \sum_l |\psi_l|^2 + J \sum_l |\psi_l - \psi_{l+1}|^2, \quad (5)$$

where ψ_l is the wave function of the carrier localized on site l , E_0 is the on-site electron (hole) energy which is determined by the affinity (ionization) potential of the base, and J describes carrier hopping between adjacent sites. The on-site energy and the hopping integral are affected by various motions of the chain. The role of vibrational degrees of freedom which are responsible for the change of the distance between subunits and the relative twist angles is well established [9,32]. As pointed out by a number of workers [8,9] the electron-phonon interaction in DNA leads to the creation of small radius polarons. We are interested here in the role of bending degrees of freedom and their coupling with charge

carriers. To be more concrete we assume that each site possesses a permanent quadrupole moment. The interaction between the charge carriers and the quadrupole moments provides on-site softening (or hardening) of bending rigidity of the chain (see Appendix A for details) which in turn may lead to the change of geometry of the chain. As is shown in Appendix A, the coupling between the charge carrier and the molecular geometry is described by the Hamiltonian

$$H_{\text{el-conf}} = -\frac{1}{2} \sum_l \chi (|\psi_{l+1}|^2 + |\psi_{l-1}|^2) \kappa_l^2, \quad (6)$$

where χ is the carrier-curvature coupling constant. The total Hamiltonian of the system can be presented as the sum

$$H = U_b + U_s + H_{\text{el}} + H_{\text{el-conf}} \quad (7)$$

The quantity

$$\nu \equiv \frac{1}{L} \sum_l |\psi_l|^2 \quad (8)$$

gives the total density of charge carriers which can move along the chain and participate in the formation of the conformational state of the system. We will neglect the interaction between electron (holes). This is legitimate when the total density of electrons (holes) in the chain ν is small. Combining Eqs. (2) and (6), we notice that the effective bending rigidity changes close the points where the electron (hole) is localized. For positive values of the coupling constant χ there is a local softening of the chain, while for χ negative there is a local hardening of the chain [33]. In what follows we assume that the chain is planar ($z_l=0$) and inextensible ($\sigma \rightarrow \infty$):

$$|\vec{r}_l - \vec{r}_{l+1}| = 1. \quad (9)$$

III. CONTINUUM APPROACH

We are interested here in the case when the characteristic size of the excitation is much larger than the lattice spacing. This permits us to replace ψ_l by the function $\psi(s)$ of the arclength s which is the continuum analog of n . Using the Euler-Mclaurin summation formula [34] we get

$$H = U_b + H_{\text{el}}, \quad (10)$$

$$U_b = \frac{1}{2} k \int_0^L \kappa(s)^2 ds, \quad (11)$$

$$H_{\text{el}} = \int_0^L \{J |\partial_s \psi|^2 - \chi \kappa(s)^2 |\psi|^2\} ds. \quad (12)$$

Being interested here in small curvature effects: $\kappa(s) \ll \kappa_{\text{max}}$, we consider the bending energy in the harmonic approximation given by Eq. (11).

A. Ground state of the chain

The electron ground state wave function $\psi(s)$ [$\psi(s)$ is real] and the shape of the chain $\vec{r}(s)$ may be obtained by minimizing the functional

$$\mathcal{E} = H_{\text{el}} + U_b \quad (13)$$

with H_{el} and U_b given by Eqs. (12) and (11) under the constraint

$$\nu = \frac{1}{L} \int_0^L \psi(s)^2 ds, \quad (14)$$

which is a continuum analog of Eq. (8). The inextensibility constraint (9) reads in the continuum limit

$$|\partial_s \vec{r}|^2 = 1. \quad (15)$$

The inextensibility constraint (15) is automatically taken into account by choosing the parametrization

$$\partial_s x(s) = \sin \theta(s), \quad \partial_s y(s) = \cos \theta(s), \quad (16)$$

where the angle $\theta(s)$ satisfies the conditions

$$\theta(s+L) = 2\pi + \theta(s) \quad (17)$$

and

$$\int_0^L \cos \theta(s) ds = \int_0^L \sin \theta(s) ds = 0 \quad (18)$$

which follow from Eq. (1). Note that, in the continuum limit, the curvature of the chain $\kappa(s)$ given by Eq. (3) can be expressed as

$$\kappa(s) = |\partial_s^2 \vec{r}(s)|. \quad (19)$$

Thus, in the frame of the parametrization (16)

$$\kappa(s) = \partial_s \theta \quad (20)$$

and the functional (13) takes the form

$$\mathcal{E} = \int_0^L \left\{ J \nu (\partial_s \varphi)^2 + \left(\frac{k}{2} - \chi \nu \varphi^2 \right) (\partial_s \theta)^2 \right\} ds, \quad (21)$$

where the rescaled function $\varphi(s) = \sqrt{\nu} \psi(s)$ which satisfies the normalization condition

$$\frac{1}{L} \int_0^L \varphi^2(s) ds = 1, \quad (22)$$

has been introduced.

The Euler-Lagrange equations for the problem of minimizing \mathcal{E} , given by Eq. (21) under the constraint (22) become

$$\partial_s^2 \varphi + \frac{\chi}{J} (\partial_s \theta)^2 \varphi - \lambda \varphi = 0, \quad (23)$$

$$\partial_s [\partial_s \theta (1 - w \varphi^2)] = 0, \quad (24)$$

where λ is the Lagrange multiplier and

$$w = \frac{2\chi\nu}{k} \quad (25)$$

is a coupling constant which characterizes the strength of the charge-curvature interaction in terms of the bending rigidity of the chain and the charge density. We are interested

in solutions of Eq. (23) subject to the periodic boundary conditions

$$\varphi(s) = \varphi\left(s + \frac{L}{n}\right), \quad (26)$$

where n is an integer which characterizes the shape of the chain (see below). Integrating Eq. (24), we get

$$\partial_s \theta = \frac{A}{1 - w\varphi^2}, \quad (27)$$

where A is an integration constant. Taking into account the condition (17) we obtain that the integration constant A is determined by the relation

$$A = \frac{2\pi}{L}I, \quad (28)$$

where the functional I is given by the relation

$$\frac{1}{I} = \frac{1}{L} \int_0^L \frac{ds}{1 - w\varphi^2}. \quad (29)$$

From Eqs. (16) and (27) we see that the shape of the chain is determined by the equations

$$\begin{aligned} x(s) &= \int_0^s \sin \theta(s') ds', & y(s) &= \int_0^s \cos \theta(s') ds', \\ \theta(s) &= \frac{2\pi}{LI} \int_0^s \frac{1}{1 - w\varphi^2(s')} ds'. \end{aligned} \quad (30)$$

B. Solution of the Euler-Lagrange equations

There are two kinds of solutions to Eqs. (23) and (27).

(i) *Circular chain.* Charge is uniformly distributed along the chain

$$\varphi = 1, \quad (31)$$

where the normalization condition (14) has been used, and the curvature of the chain is constant

$$\kappa(s) \equiv \partial_s \theta = \frac{A}{1 - w}. \quad (32)$$

This case corresponds to a circular chain

$$x = R \sin \frac{s}{R}, \quad y = -R \cos \frac{s}{R}. \quad (33)$$

The radius R of the circle can be obtained by putting Eq. (32) into the boundary condition (17). As a result we have

$$R = \frac{L}{2\pi}. \quad (34)$$

The energy of the circular chain is thus

$$\mathcal{E}_{\text{circ}} = \frac{2\pi^2}{L} k(1 - w). \quad (35)$$

(ii) *Polygonally deformed chain.* Let us consider now the case of spatially nonuniform distributed electrons. Inserting Eqs. (27)–(29) into Eq. (21) we get

$$\mathcal{E} = J\nu \int_0^L (\partial_s \varphi)^2 ds + \frac{2\pi^2 k}{L} I. \quad (36)$$

We restrict our analytical consideration to the case when the charge-curvature coupling is weak and/or the charge density is low: $w \ll 1$. Expanding the functional I in terms of the small parameter w we obtain from Eq. (36)

$$\mathcal{E} = \frac{2\pi^2 k}{L(1+w)} + J\nu \int_0^L \left\{ (\partial_s \varphi)^2 - \frac{G\nu}{R^2} \varphi^4 - w \frac{G\nu}{R^2} \varphi^6 \right\} ds, \quad (37)$$

where

$$G = \frac{2\chi^2}{Jk(1+w)^2} \quad (38)$$

is an effective nonlinear parameter. For small w one can neglect the last term in Eq. (37) and the Euler-Lagrange equation for the functional (37) then takes the form

$$\partial_s^2 \varphi + 2 \frac{G\nu}{R^2} \varphi^3 - \lambda \varphi = 0. \quad (39)$$

Straightforward calculations show that Eq. (39) has a solution of the form

$$\varphi = R \sqrt{\frac{\lambda}{(2-m)G\nu}} \operatorname{dn} \left(\sqrt{\frac{\lambda}{(2-m)}} s \middle| m \right), \quad (40)$$

where $\operatorname{dn}(u|m)$ is the Jacobi elliptic function with the modulus m [34]. Inserting Eq. (40) into the boundary condition (26) and the normalization condition (22), we find that the Lagrange multiplier λ and the modulus m are determined by the equations

$$\sqrt{\frac{\lambda}{(2-m)}} \frac{L}{n} = 2K(m), \quad (41)$$

$$G\nu = \frac{n^2}{\pi^2} K(m)E(m) \quad (42)$$

and the charge distribution along the chain is given by

$$\varphi = \sqrt{\frac{K}{E}} \operatorname{dn} \left(\frac{2nK}{L} s \middle| m \right), \quad (43)$$

where $K(m)$ and $E(m)$ are the complete elliptic integrals of the first kind and the second kind, respectively [34].

The curvature of the chain is given by the equation

$$\begin{aligned} \kappa(s) \equiv \partial_s \theta &\approx \frac{1}{R} \left[1 + w \frac{K}{E} \operatorname{dn}^2 \left(\frac{2nsK}{L} \middle| m \right) \right. \\ &\left. + w^2 \frac{K^2}{E^2} \operatorname{dn}^4 \left(\frac{2nsK}{L} \middle| m \right) \right]. \end{aligned} \quad (44)$$

Integrating Eq. (44) and neglecting terms of the order w^2 , we get

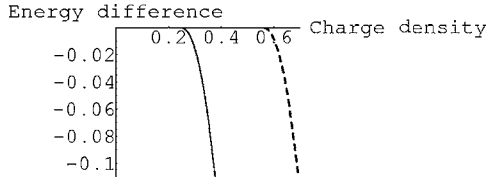


FIG. 2. The normalized energy difference Δ_n from Eq. (49) for the ellipselike $n=2$ (solid line) and triagonlike chain $n=3$ (dashed line) with $2\chi=4$ $J=k$.

$$\theta(s) = \frac{2\pi}{L} I \left(s + w \frac{L}{2nE} E(\alpha|m) \right), \quad (45)$$

where $E(\alpha|m)$ is the incomplete elliptic integral of the second kind, and $\alpha = am \left(\frac{2nK}{L} s | m \right)$ is the amplitude function [34]. By using the Fourier expansion for the amplitude function for small m we obtain from Eq. (45)

$$\theta(s) \approx \frac{2\pi}{L} (1+w)Is + \frac{w}{4n} Im \sin \left(\frac{2n\pi}{L} s \right). \quad (46)$$

Inserting Eq. (46) into the closure condition (18), we find that it is satisfied for $n \geq 2$. Equations (30) and (46) describe a polygon: for $n=2$ it is an elliptically deformed chain, while for $n=3$ it has a triangular shape (see Fig. 1). We see from Eqs. (43) and (44) that the polygon structure is a result of the self-consistent interaction between electrons and bending degrees of freedom: extrema of the curvature and of the charge density correlate: in the case of the softening electron-curvature interaction ($\chi > 0$) maxima of curvature and charge density coincide, while in the case of the hardening interaction ($\chi < 0$) the minima of the curvature coincide with the maxima of the charge density. Equation (42) shows that, for a given value of the nonlinear parameter G , the n -gon structure appears when the charge density exceeds the threshold value ν_n :

$$\nu > \nu_n \equiv \frac{n^2}{4G}. \quad (47)$$

The energy difference between the n -gon structure and the circular chain is given by the expression

$$\mathcal{E}_n - \mathcal{E}_{\text{circ}} = \frac{4\pi^2}{3L} \frac{GJ\nu^2}{E^2} [3E^2 - (2-m)EK - (1-m)K^2]. \quad (48)$$

The normalized energy difference

$$\Delta_n = \frac{\mathcal{E}_n - \mathcal{E}_{\text{circ}}}{\mathcal{E}_{\text{circ}}} \quad (49)$$

for $n=2,3$ versus the charge density is shown in Fig. 2. We note that when the charge density is above the critical value the deformed structure with spatially inhomogeneous charge distribution is energetically more favorable than the circular system with a uniformly distributed charge. The state with elliptically deformed chain $n=2$ is the most energetically preferable.

Note also that our analytical approach was based on the assumption that $w\varphi^2 \ll 1$. Taking into account Eq. (43), this means that it is legitimate to consider not too sharp distributions which correspond to $wK(m) \ll 1$ or $m \ll 1 - \exp\{-0.72/w\}$.

C. Estimates

As an example, let us consider the possibility of the creation of a deformed structure with spatially inhomogeneous charge distribution in closed DNA-like polymers where each subunit is modeled as an ellipsoid with a quadrupole moment $Q_{\alpha\beta}$. The coupling between a charge carrier (an extra electron or hole) and curvature is due to the charge-quadrupole interaction

$$\chi = \frac{e\Delta Q}{a^3}, \quad (50)$$

where the quantity $\Delta Q = Q_\tau - Q_\nu$ characterizes the anisotropy of the charge distribution in the subunit (see Appendix A for details). By using the esu units for the quadrupole moments $\Delta Q = q10^{-26}$ esu cm^2 , where q is a dimensionless quadrupole anisotropy parameter, and assuming that the distance between subunits a is given by $a = (3.5-4.5)10^{-8}$ cm (as in DNA molecules), from Eq. (50) we get

$$\chi = (0.03 - 0.07)q \text{ eV}. \quad (51)$$

The bending rigidity of the chain k can be expressed as [35]

$$k = l_p k_B T, \quad (52)$$

where l_p is the persistence length in units of chain period, T is the temperature, and k_B is the Boltzmann constant. Following estimates presented in Ref. [10] we chose $J \approx 0.1$ eV. Introducing Eqs. (51) and (52) into Eq. (38) for $k_B T \approx 0.02$ eV (room temperature), we get

$$G = (1-5) \frac{q^2}{l_p}, \quad (53)$$

where we have neglected $w \ll 1$ in the denominator of Eq. (38). Thus, for a chain which has a persistence length in the interval $l_p = 100-200$ (DNA-like molecules) and which consists of subunits with the quadrupole moment anisotropy $q = 10-30$ (e.g., aromatic molecules – uracil-glycine complexes [36]) we find that $G \sim 1-25$. This means that the threshold condition (47) may be fulfilled for relatively low concentration of charge carriers in the chain.

IV. NUMERICAL STUDIES

To check our results we have performed also several numerical studies. To this end we carried out the dynamical simulations of the equations

$$\eta \frac{d}{dt} \vec{r}_l = - \frac{\partial H}{\partial \vec{r}_l}, \quad (54)$$

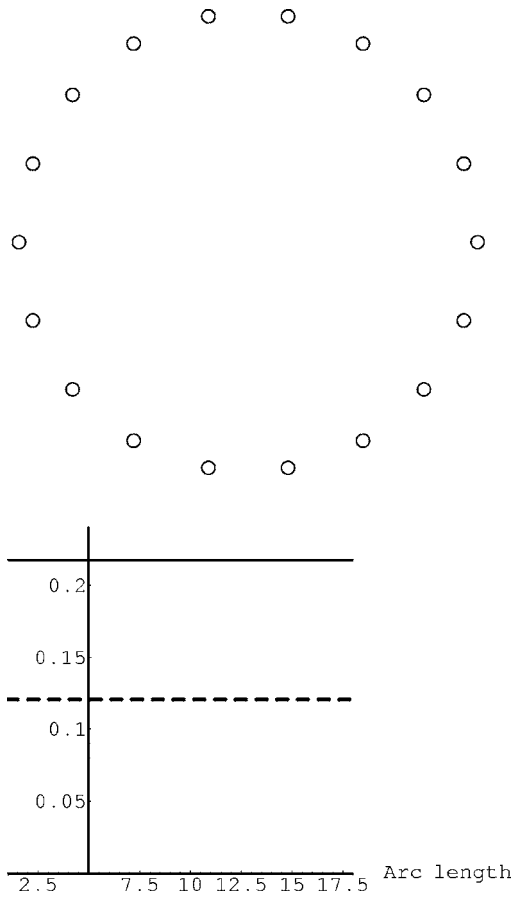


FIG. 3. The top panel shows the initial shape of the chain; the bottom panel shows the initial charge (solid line) and curvature (dashed line) distribution along the chain.

$$i \frac{d}{dt} \psi_l = - \frac{\partial H}{\partial \psi_l^*} \quad (55)$$

with the Hamiltonian H being defined by Eqs. (6) and (7). Thus the conformational dynamics is considered in an overdamped regime with the friction coefficient η . Then we took as our starting configurations systems involving the electric charge density of (almost) the same magnitude (ψ_l) at all points (we broke the symmetry by increasing the density at one point of the chain by 1%). Initially, all the lattice points were placed at symmetric points on the circle of an appropriate radius (see Fig. 3). We performed such simulations for several values of the charge density. Due to the absorption the energy of the system was decreasing during the evolution and the system was evolving towards a minimum. At the same time the points of the chain were moving from their initial to their new positions.

We considered both the cases of the hardening and softening of the electron-curvature interaction. In the case of a hardening electron-curvature interaction ($\chi < 0$) a typical final distribution of the chain points is shown in Fig. 4. The charge density and the curvature distributions are in full agreement with the results of our analytical considerations: the curve is more flat where the density of the electrons is maximal. In fact, the ellipselike shape is rather robust as it

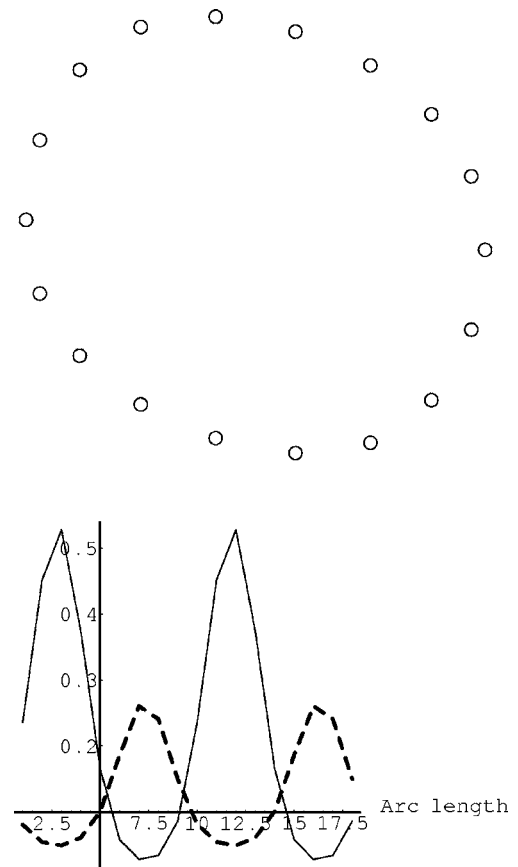


FIG. 4. The top panel shows the equilibrium shape of the chain and the bottom panel shows the charge distribution (solid line) and curvature variation (dashed line) along the chain in the case of hardening electron-curvature interaction with $\nu=0.22$, $\chi=-2$, $k=1$, $J=0.4$.

arises for a large range of parameters (of the strength of the hardening electron-curvature interaction and of the anharmonicity coefficient κ_{\max}).

Complexes with a softening electron-curvature interaction are much more flexible. Their equilibrium shape depends drastically both on the anharmonicity and on the charge density. Figures 5 and 6 demonstrate how drastically the shape of the complex and the charge distribution along the chain can change as a function of the total charge density ν : increasing the total charge by 5% can lead to the localisation of almost the whole charge of the system at one place.

In our numerical work we also studied the stability of our “final” field configurations, i.e., the configurations which we thought the system was settling at. This we studied by perturbing the system. Such perturbations were introduced in two stages. First we changed the electric charge of the configuration by multiplying all “final” values of the electric charge by a constant factor μ ; this had the effect of changing the energy of the system. Then we performed the new minimization and, when the system appeared to have settled at the new “final” configuration, we changed back its ψ_l by a new multiplication by $1/\mu$. As $\sum_l |\psi_l|^2$ is conserved during the evolution, the final system had the same value of it as the original “unperturbed” fields. The results of the further minimisation were then compared with the original “final” fields.

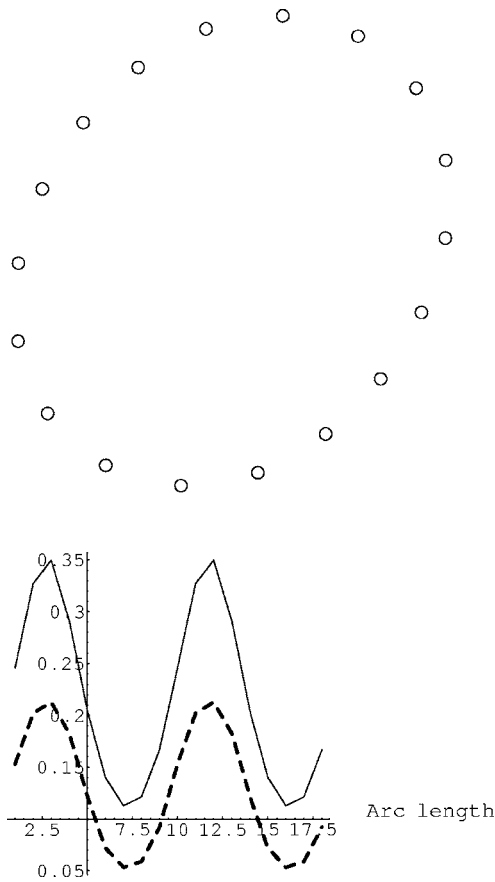


FIG. 5. The top panel shows the equilibrium shape of the chain and the bottom panel shows the charge distribution (solid line) and curvature variation (dashed line) along the chain in the case of softening electron-curvature interaction with $\nu=0.22$, $\chi=2.15$, and $k=J=1$.

When we applied this technique to our field configuration shown in Fig. 6 we found that the system was really unchanged by this perturbation; in fact the perturbation led to an overall rotation of the system by one lattice point, but the sequence of values of the fields was essentially the same thus showing the stability of the found minimum.

V. EFFECTS OF INTERCOMPLEX INTERACTION

The aim of this section is to investigate how the interaction between complexes influences the shape. We will consider the system which is described by the Hamiltonian

$$\mathcal{H} = \sum_j \mathcal{E}_j + \frac{1}{2} \sum_{ij} U_{ij}, \quad (56)$$

where \mathcal{E}_j is the energy of the j th aggregate which is given by Eq. (21) with φ replaced by φ_j and θ replaced by θ_j , and U_{ij} is the interaction energy between particles. The latter we will take in the form of the Gay-Berne potential [37] which is a generalization of the Lennard-Jones 12-6 potential and is widely used to study translational and orientational ordering in systems of aspherical molecules. We consider small deviations from the ringlike structure of aggregates and so we

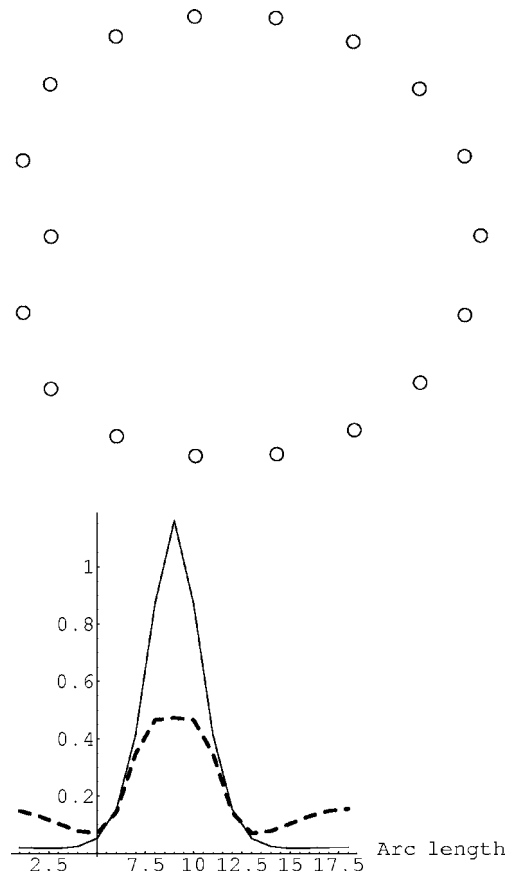


FIG. 6. Same as Fig. 5 with $\nu=0.23$, $\chi=2.15$, $k=J=1$.

neglect the difference of the well depths for side-to-side and end-to-end configurations. In this case the Gay-Berne potential between two parallel uniaxial molecules is given by

$$U_{ij} \equiv U(\vec{r}_{ij}) = \frac{U_0}{\sqrt{1-\zeta^2}} \left[\left(\frac{\sigma_0}{r_{ij} + \sigma(\hat{r}_{ij}) + \sigma_0} \right)^{12} - \left(\frac{\sigma_0}{r_{ij} + \sigma(\hat{r}_{ij}) + \sigma_0} \right)^6 \right], \quad (57)$$

where $\vec{r}_{ij} = r_{ij} \hat{r}_{ij}$ is the interparticle vector and

$$\sigma(\hat{r}_{ij}) = \sigma_0 \left[1 - \frac{2\zeta}{1+\zeta} (\hat{r}_{ij} \cdot \vec{e})^2 \right]^{-1/2} \quad (58)$$

is the anisotropy parameter where \vec{e} is a unit vector specifying the axes of symmetry. The anisotropy coefficient ζ is determined by the lengths of the major and minor axes σ_{\parallel} and σ_{\perp}

$$\zeta = \frac{\sigma_{\parallel}^2 - \sigma_{\perp}^2}{\sigma_{\parallel}^2 + \sigma_{\perp}^2} \quad (59)$$

and σ_0 gives a characteristic length scale while U_0 determines the intensity of the interaction.

The centers of densely packed circular aggregates of the radius R create a two-dimensional triangular lattice $\vec{r}_j = j_1 \vec{a}_1 + j_2 \vec{a}_2$ [$j \equiv (j_1, j_2)$, $j_1, j_2 = 0, \pm 1, \pm 2, \dots$] with the

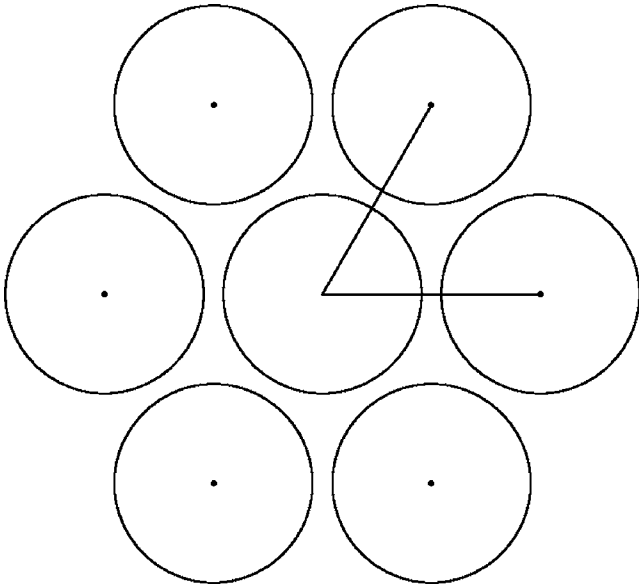


FIG. 7. Arrangement of densely packed ringlike aggregates.

basic vectors $\vec{a}_1=l(1,0)$ and $\vec{a}_2=l(1/2, \sqrt{3}/2)$, where l is the lattice constant (see Fig. 7). Being elliptically deformed in such a way that the major axes of all aggregates are parallel to the x axis, the centers of densely packed elliptical aggregates create a lattice $\vec{r}_j=j_1\vec{b}_1+j_2\vec{b}_2$ with the basic vectors $\vec{b}_1=l(1+u,0)$ and $\vec{b}_2=l[1/2(1+u), \sqrt{3}/2(1-u)]$ (see Fig. 8), where the parameter u is given by

$$u = \frac{\sigma_{\parallel} - \sigma_{\perp}}{\sigma_{\parallel} + \sigma_{\perp}}. \quad (60)$$

Now we study the ground state of this system by using a trial function approach. We assume that this state is spatially homogeneous and relying on the results of the previous section, we assume that the electron trial function and the trial curvature can be taken in the form

$$\varphi_j = \left[\cos \alpha + \sqrt{2} \sin \alpha \cos\left(\frac{2s}{R}\right) \right], \quad (61)$$

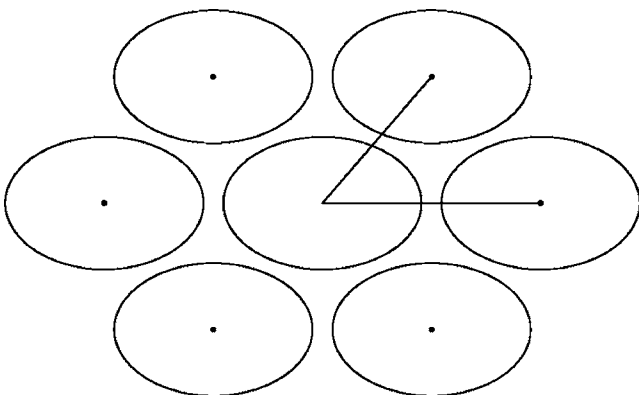


FIG. 8. Arrangement of densely packed ellipselike aggregates.

$$\partial_s \theta_j = \frac{1}{R} \left[1 + \gamma \cos\left(\frac{2s}{R}\right) \right]. \quad (62)$$

The functions (61) and (62) can be considered as a truncated Fourier expansion of the solutions (40) and (44) in which the coefficients α and γ are variational parameters and R is the radius of the cylindrically symmetric aggregate. The function (61) satisfies both the periodicity condition (26) and the number of particles constraint (14). In the limit $\gamma < 1$ the shape of the curve with the curvature given by Eq. (62) is parametrically determined by the expressions

$$\begin{aligned} x(s) &= R \left[\left(1 + \frac{\gamma}{4} \right) \cos\left(\frac{s}{R}\right) + \frac{\gamma}{12} \cos\left(\frac{3s}{R}\right) \right], \\ y(s) &= R \left[\left(1 - \frac{\gamma}{4} \right) \sin\left(\frac{s}{R}\right) + \frac{\gamma}{12} \sin\left(\frac{3s}{R}\right) \right]. \end{aligned} \quad (63)$$

Thus the lengths of the major and minor axes of the curve (63) are given by

$$\sigma_{\parallel} = R \left(1 + \frac{\gamma}{3} \right), \quad \sigma_{\perp} = R \left(1 - \frac{\gamma}{3} \right) \quad (64)$$

and comparing Eqs (60) and (64), we see that $u = \gamma/3$.

Inserting Eqs. (61) and (62) into Eqs. (56), (21), and (57) for an energy per aggregate we get

$$\frac{\mathcal{H}}{N_a} = \mathcal{E}_{\text{tr}} + U, \quad (65)$$

where

$$\begin{aligned} \mathcal{E}_{\text{tr}} &= \frac{\pi k}{R} \left\{ 1 + \frac{\gamma^2}{2} - \frac{1}{8} \xi \nu [8 + 5\gamma^2 - \gamma^2 \cos(2\alpha)] \right. \\ &\quad \left. + 8\sqrt{2} \sin(2\alpha) \right\} + \frac{4J}{k} \nu \sin^2 \alpha \end{aligned} \quad (66)$$

is the energy of an isolated aggregate, and

$$U = \sum_{j=0}^5 U(\vec{\Delta}_j) \quad (67)$$

is the energy due to the interaction between aggregates in the lattice. In Eq. (67) the function $U(\vec{\Delta}_j)$ is given by Eqs. (57) and (58) with $\vec{e}=(1,0)$ and vectors $\vec{\Delta}_j = \sigma_0 \left[\left(1 + \frac{\gamma}{3} \right) \cos\left(\frac{\pi j}{3}\right), \left(1 - \frac{\gamma}{3} \right) \sin\left(\frac{\pi j}{3}\right) \right]$ connect nearest and next-nearest neighbors of the lattice. The interaction energy (67) has a minimum at $l=2^{1/6}\sigma_0$, $\gamma=0$ which corresponds to a system of densely packed circular aggregates. Expanding the function (67) in the vicinity of this point, in powers of the variational parameter γ , we get

$$U = -\frac{3}{2} U_0 + c U_0 \gamma^2 + \dots, \quad (68)$$

where the numerical coefficient $c \approx 2.05$. According to the variational principle we should satisfy the equations

$$\partial_{\alpha} \mathcal{E}_{\text{tr}} = 0, \quad (69)$$

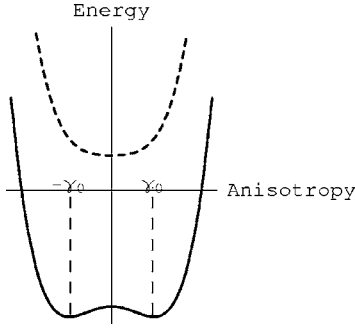


FIG. 9. Energy per aggregate [Eq. (65)] as a function of the trial anisotropy parameter γ for the charge density below the threshold (dashed) and above the threshold (solid).

$$\partial_{\gamma}(\mathcal{E}_{\text{tr}} + U) = 0. \quad (70)$$

From Eq. (69) we get

$$\tan(2\alpha) = \frac{8\sqrt{2}k\xi}{32J - k\xi\gamma^2} \gamma. \quad (71)$$

Inserting Eq. (71) into Eq. (66) and expanding it in terms of γ we obtain that

$$\mathcal{E}_{\text{tr}} = \mathcal{E}_{\text{circ}} + \frac{\pi k}{2R} \left(1 - \frac{\nu}{\nu_{\text{cr}}}\right) \gamma^2 + B\gamma^4 + \dots, \quad (72)$$

where

$$\nu_{\text{cr}} = \frac{k}{2\chi} \frac{J}{J + \chi} \quad (73)$$

is the critical charge density and the notation

$$B = \frac{\pi}{16R} \frac{\chi^3 \nu}{J^3} (2\chi - J)$$

is introduced. Thus in the framework of the variational approach the energy of a single complex has a single minimum at $\gamma=0$ when $\nu < \nu_{\text{cr}}$ and in this case the aggregate has a ringlike shape. When $\nu > \nu_{\text{cr}}$ and $2\chi > J$ the energy (72) possesses two equivalent minima with $\pm\gamma_0$ ($\gamma_0 \neq 0$) (see Fig. 9). As seen from Eqs. (63) the finite value of γ_0 implies that the aggregate is elliptically deformed either along the x axis (when $\gamma > 0$) or along the y axis (when $\gamma < 0$). Note that in the limit $\chi \gg J$, ν_{cr} coincides with ν_2 given by Eq.(47). Combining (68) and (72) we see that the interaction between aggregates modifies the condition for appearance of the low-symmetry form. Indeed, even in the case when $\nu > \nu_{\text{cr}}$ (an isolated aggregate has an ellipselike shape) in the condensed phase of aggregates for strong enough interaggregate interaction we may have an inequality

$$\nu < \nu_{\text{cr}} \left(1 + \frac{2cU_0}{\pi k} R\right) \quad (74)$$

which means that interacting aggregates are ringlike and create a densely packed crystallic structure with the group symmetry D_{6h} (see Fig. 7). When

$$\nu > \nu_{\text{cr}} \left(1 + \frac{2cU_0}{\pi k} R\right) \quad (75)$$

the ellipselike shape survives in the condensed phase which has a rectangular unit cell and transforms in accordance with the group symmetry D_{2h} (see Fig. 8). There are two equivalent types of arrangement in the low-symmetry phase when the aggregates are elliptically deformed either along the x axis (when $\gamma > 0$) or along the y axis (when $\gamma < 0$). In accordance with this, the condensed phase of the aggregates must have a domain structure, i.e., it must consist of various regions in which the direction of long axes are different.

VI. APPLICATIONS

A. Application to bacteriochlorophyll a complexes

As mentioned in the Introduction, the isolated light-harvesting rings can deviate from the ideally circular structure of the complex in crystals. For example, in contrast to the cylindrical crystal structure with a diameter of 6.8 nm, the shape of an isolated LH2 complex from bacteria *Rhodobacter spheroides* 2.4.1 is an oblate plate with an eccentricity $\epsilon=0.59$ [27]. It was conjectured in Ref. [24] that the extremely dense packing of LH2 in crystals causes the cylindrical symmetry of the complexes. Based on the resonance Raman, mutagenesis, and atomic microscopy approaches [28,38,39], it has been proposed that a network of hydrogen bonds stabilizes the structure of light-harvesting complexes. We suggest that the flexible geometry of these complexes is due to the interaction between proton-assisted mobile defects and the bending degrees of freedom. The quantum description of Bjerrum and polarization defects based on a tight-binding Hubbard-like Hamiltonian was presented in Ref. [40]. Recently a model, in which a tight-binding electronic Hamiltonian was used for the dynamics of defects on hydrogen-bonded chains [41,42]. Applying the above-developed theory to the case of flexible light-harvesting complexes [this means that $\psi_n(t)$ is now the wave function of the defect at the site n of the hydrogen-bonded network], we obtain a qualitative explanation of these transformations. It has shown that in the presence of sufficiently strong charge-curvature interaction an isolated complex has an ellipselike shape while the interaction between complexes in the form of an anisotropic Gay-Berne potential stabilizes the ringlike shapes of the complexes. However, if the intensity of the intercomplex interaction is less than some threshold value [see Eqs. (68) and (72)] the noncircular shape of the complex is preserved in the condensed phase. The model is too simplified for quantitative predictions for light-harvesting complexes but we believe that it contains interesting physics which should be important for further studies of such systems.

B. Exciton spectra of polygonally deformed chains

One can expect that the polygonal deformation of chains may be established by observing their fluorescence from polarized light excitation. A link between a geometrical deformation and the spectroscopic properties has recently been

provided by measuring fluorescence-excitation spectra of light-harvesting complexes from *Rhodospseudomonas acidophila* in Refs. [23–25]. Measurements of the anisotropic properties of the absorption of isolated LH2 complexes from bound to mica surfaces [25], the fluorescence-excitation spectra of individual LH2 complexes from bacteria *Rhodospseudomonas acidophila* [23,24,26] showed that the complexes are generally not cylindrically symmetric but reveal a deformation of the circular complex into an elliptical shape. The properties of exciton states of elliptically deformed LH2 complexes were considered in Ref. [26]. It was concluded that an elliptical shape with the eccentricity 0.58 can explain the splitting of exciton states and other features of the spectra of individual LH2 complexes.

Exciton spectra of polygonally deformed chains also provide useful information on the geometry of the system. There are two types of exciton states in closed chains: even states $\langle C_k |$ and odd states $\langle S_k |$ (the parameter $k=0,1,\dots,(L/2-1),L/2$ gives the number of nodes of the exciton wave function on the half period). In cylindrically symmetric aggregates the states with $k=1,\dots,(L/2-1)$ are doubly degenerate. Under polygonal shape transitions circle $\rightarrow n$ -gon the exciton states experience an energetic shift $\Delta_n(k)$ and a doublet splitting $\delta_n(k)$. Using the theory developed above, in the framework of the zeroth-order perturbation, one can obtain (see Appendix B for details) that

$$\Delta_n(k) \approx -M \frac{w^2}{4R^2} \left(\frac{4}{n^2} G\nu - 1 \right) \cos \frac{2\pi k}{L}. \quad (76)$$

The degeneracy of the exciton levels is removed for states with $2k=nj$, ($j=1,2,\dots$). This means, in particular, that all exciton states (B9) of the elliptically deformed chain ($n=2$) split and the maximal splitting takes place for the state with $k=1$. In the limit of small w and m this splitting is given by

$$\delta_2(1) = M \frac{mw}{2R^2} \cos \frac{2\pi}{L}, \quad (77)$$

where m is given by Eq. (B16). When $n=4$ the states with even k split while the states with odd k remain degenerate. For polygonally deformed chains with odd number of sides (i.e., $n=3,5,\dots$) in the order of approximation under consideration $\delta_n(k)=0$ all exciton states remain doubly degenerate.

VII. CONCLUSIONS AND DISCUSSION

In this paper, we have investigated the role of the charge-curvature interaction on the formation of the ground state of closed semiflexible molecular chains. We have found that the coupling between charge carriers and the bending degrees of freedom of the chain can induce a local softening or hardening of chain bonds, i.e., the effective bending rigidity of the semiflexible chain changes as the density of charge changes along the chain. When the charge density and/or the strength of the charge-curvature coupling exceed a threshold value, the spatially uniform distribution of the charge along the chain and the circular, cylindrically symmetric shape of the chain become unstable. In this case the ground state of the system is characterized by a spatially nonuniform charge dis-

tribution along the chain and the chain takes on an ellipselike (or in general polygonlike) form.

These results were obtained by using the mean-field approach where thermal fluctuations are ignored and strictly speaking, this approach is valid only for low temperatures. However, this case is also experimentally relevant. As an example one can recall experiments in Refs. [23,24], where the fluorescence-excitation spectra of individual light-harvesting complexes at 1.2 K were measured and C_2 geometrical deformations were found.

In the case of high temperatures the role of fluctuations may be crucial. For example, in Ref. [19] the effects of thermal fluctuations on buckling in polyelectrolytes were studied and it was shown that in polyelectrolytes with attractive intrachain interactions the thermal fluctuations destroy the buckling instability and convert it into a collapse. One can also expect that the thermal fluctuations are particularly important for closed chains with a softening charge-curvature interaction because the presence of charge in this case facilitates the buckling and collapse of the chain (see, e.g., Ref. [18]). Contrary to this, in the systems where the presence of charge *hardens* the local chain stiffness, the charge-curvature interaction counteracts the collapse of the chain and one can expect that the mean-field picture survives. We plan to investigate how the thermal fluctuations effect the mean-field picture in a future work.

ACKNOWLEDGMENTS

Yu. B. G. would like to thank L. Valkunas for attracting attention to the problem of structural deformations of light-harvesting complexes. Yu.B.G. and W.J.Z. thank L. Brizhik, A. Eremko, and B. Piette for interest and helpful discussions. Yu.B.G. acknowledges the Civilingeniør Frederik Christiansens Almennyttige Fond for financial support, MIDIT, SNF Grant No. 21-02-0500, and the research center of quantum medicine “Vidguk.” He also thanks the Department of Physics, the Technical University of Denmark for hospitality.

APPENDIX A

The aim of this appendix is to derive an explicit form of the electron-conformation interaction. We assume that each l th chain unit possesses a quadrupole moment which is characterized by the tensor $Q_l^{\alpha\beta}$ ($\alpha, \beta=x, y, z$). Then the interaction between an electron and chain units takes the form

$$H_{\text{int}} = \sum_{l,l'} V_{ll'} |\psi_l|^2, \quad (A1)$$

where the matrix element $V_{ll'}$ describes a charge-quadrupole interaction between an electron which occupies the site n in the chain and the group at the site n'

$$V_{ll'} = \sum_{\alpha\beta} \frac{e Q_n^{\alpha\beta} (\vec{r}_l - \vec{r}_{l'})_\alpha (\vec{r}_l - \vec{r}_{l'})_\beta}{|\vec{r}_l - \vec{r}_{l'}|^5}. \quad (A2)$$

We assume that the quadrupole moment tensor $Q_n^{\alpha\beta}$ is diagonal in the local frame of reference which is determined by the triad $(\vec{t}_n, \vec{v}_n, \vec{z})$, where

$$\vec{\tau}_l = \frac{\vec{r}_{l+1} - \vec{r}_l}{|\vec{r}_{l+1} - \vec{r}_l|} \equiv \frac{1}{|\vec{r}_{l+1} - \vec{r}_l|} (x_{l+1} - x_l, y_{l+1} - y_l, 0) \quad (\text{A3})$$

is the unit tangent vector,

$$\vec{v}_l = \hat{z} \times \frac{\vec{r}_{l+1} - \vec{r}_l}{|\vec{r}_{l+1} - \vec{r}_l|} \equiv \frac{1}{|\vec{r}_{l+1} - \vec{r}_l|} (-y_{l+1} + y_l, x_{l+1} - x_l, 0) \quad (\text{A4})$$

is the normal to the chain at the point l , and \hat{z} is the unit vector perpendicular to the xy plane. In this case the interaction (A2) takes the form

$$V_{ll'} = \frac{e}{|\vec{r}_l - \vec{r}_{l'}|^5} \{Q_\tau [\vec{\tau}_l \cdot (\vec{r}_l - \vec{r}_{l'})]^2 + Q_\nu [\vec{v}_l \cdot (\vec{r}_l - \vec{r}_{l'})]^2\}, \quad (\text{A5})$$

where Q_τ (Q_ν) is the tangential (normal) component of the quadrupole moment. Let us consider the nearest-neighbor approximation. Taking into account that

$$(\vec{r}_{l+2} - \vec{r}_{l+1}) \cdot (\vec{r}_{l+1} - \vec{r}_l) = a^2 \left(1 - \frac{1}{2} \kappa_{l+1}^2\right) \quad (\text{A6})$$

and

$$\begin{aligned} \hat{z} \times (\vec{r}_{l+2} - \vec{r}_{l+1}) \cdot (\vec{r}_{l+1} - \vec{r}_l) &= \frac{1}{2} [(x_{l+2} - 2x_{l+1} + x_l)(y_{l+2} - y_l) \\ &\quad + (y_{l+2} - 2y_{l+1} + y_l)(x_{l+2} - x_l)] \\ &\approx a^2 \kappa_{l+1}, \end{aligned} \quad (\text{A7})$$

where a discrete analog of the Frenet formula

$$\vec{\tau}_{l+1} - \vec{\tau}_l = -\kappa_l \vec{v}_l \quad (\text{A8})$$

and approximate identity

$$(x_{l+2} - x_l)(x_{l+1} - x_l) + (y_{l+2} - y_l)(y_{l+1} - y_l) \approx 2a^2$$

were used, we obtain that

$$V_{ll+1} = \frac{eQ_\tau}{a^3} - \frac{e(Q_\tau - Q_\nu)}{a^3} \kappa_{l+1}^2 + O(\kappa^4). \quad (\text{A9})$$

In the same way

$$V_{ll-1} = \frac{eQ_\tau}{a^3} - \frac{e(Q_\tau - Q_\nu)}{a^3} \kappa_{l-1}^2 + O(\kappa^4). \quad (\text{A10})$$

Introducing Eqs. (A9) and (A10) into Eq. (A1) we get

$$H_{\text{int}} = -\frac{1}{2} \sum_l \chi |\psi_l|^2 (\kappa_{l+1}^2 + \kappa_{l-1}^2), \quad (\text{A11})$$

where we have omitted a constant term and

$$\chi = \frac{e(Q_\tau - Q_\nu)}{a^3}. \quad (\text{A12})$$

In the case when the chain units are axially symmetric and

$$Q_\tau = Q_\nu = Q$$

the nearest neighbors do not contribute to the charge-curvature interaction. We should take into account the effect

due to the next-neighbor coupling and as a result we obtain the charge-curvature interaction in the form (A11) with the coupling constant χ in the form

$$\chi = -\frac{3}{32} \frac{eQ}{a^3}. \quad (\text{A13})$$

APPENDIX B

The aim of this appendix is to show how the exciton spectra of closed molecular chains change upon a polygonal deformation. According to the theory of molecular excitons [33] the exciton Hamiltonian of the chain has the form

$$H_{\text{exc}} = E_0 \sum_{l=1}^L B_l^\dagger B_l + \sum_{l,l'=1}^L M_{ll'} B_l^\dagger B_{l'}. \quad (\text{B1})$$

Here, B_l^\dagger (B_l) is the creation (annihilation) operator of the electronic excitations on the subunit l , E_0 is the excitation energy, $M_{ll'}$ is the matrix element of the excitation transfer from the subunit l to the subunit l' which we consider in the dipole-dipole approximation

$$M_{ll'} = \frac{\vec{d}_l \cdot \vec{d}_{l'}}{|\vec{r}_l - \vec{r}_{l'}|^3} - 3 \frac{[\vec{d}_l \cdot (\vec{r}_l - \vec{r}_{l'})][\vec{d}_{l'} \cdot (\vec{r}_l - \vec{r}_{l'})]}{|\vec{r}_l - \vec{r}_{l'}|^5}, \quad (\text{B2})$$

where \vec{d}_l is the transition dipole moment from the ground state $|gr\rangle$ to the excited state $|l\rangle \equiv B_l^\dagger |gr\rangle$ of the subunit l . Taking into account that in the local frame of reference $(\vec{\tau}_l, \vec{v}_l)$ the transition dipole moment can be presented in the form

$$\vec{d}_l = d_\tau \vec{\tau}_l + d_\nu \vec{v}_l, \quad (\text{B3})$$

where d_τ (d_ν) are the tangential (normal) projections of the dipole moment and restricting ourselves to the nearest-neighbor transfer, from Eqs. (B3) and (B2) we obtain that the exciton Hamiltonian of the deformed chain has the form

$$H_{\text{exc}} = E_0 \sum_{l=1}^L B_l^\dagger B_l + M \sum_{l=1}^L \left\{ \left(1 - \frac{1}{2} \kappa_l^2\right) B_l^\dagger B_{l-1} + \text{H. c.} \right\}, \quad (\text{B4})$$

where the parameter

$$M = \frac{(d_\nu^2 - 2d_\tau^2)}{a^3}$$

gives the strength of the excitation transfer.

A circular chain. It is clear from Eq. (B3) that the curvature is constant along the chain and

$$\kappa_l = \frac{1}{R} = \frac{2\pi}{L}. \quad (\text{B5})$$

There are two sets of exciton eigenstates: even eigenfunctions

$$|C_k\rangle = \sqrt{\frac{2}{L}} \sum_{l=1}^L \cos\left(\frac{2\pi kl}{L}\right) |l\rangle \quad (\text{B6})$$

with $k=0, 1, \dots, (L/2-1), L/2$, and odd eigenfunctions

$$|S_k\rangle = \sqrt{\frac{2}{L}} \sum_{l=1}^L \sin\left(\frac{2\pi kl}{L}\right) |l\rangle \quad (\text{B7})$$

with $k=1, \dots, (L/2-1)$. Both types of exciton eigenstates have the energy

$$E_k = E_0 + 2M \left(1 - \frac{2\pi^2}{L^2}\right) \cos\left(\frac{2\pi k}{L}\right). \quad (\text{B8})$$

Thus in the circular chain the eigenvalues with

$$k = 1, \dots, (L/2 - 1) \quad (\text{B9})$$

are doubly degenerate.

A polygonally deformed chain. From Eq. (B4) we see that the excitations in a polygonally deformed chain experience a perturbation which has the form

$$H_{\text{pert}} = \frac{1}{2} M \sum_l \left(\frac{1}{R^2} - \kappa_l^2 \right) B_l^\dagger B_{l-1}, \quad (\text{B10})$$

where the curvature κ_l takes the form of Eq. (44) with $s \rightarrow l$:

$$\kappa_l = \frac{1}{R} \left[1 + w \frac{K}{E} dn^2 \left(\frac{2nlK}{L} \middle| m \right) + w^2 \frac{K^2}{E^2} dn^4 \left(\frac{2nlK}{L} \middle| m \right) \right]. \quad (\text{B11})$$

Under the influence of the perturbation (B10) the exciton levels in a n -gon chain shift and split and their energy takes the form

$$E_{\pm}(k) = E_k + \Delta_n(k) \pm \frac{1}{2} \delta_n(k). \quad (\text{B12})$$

In the zeroth-order perturbation theory the exciton energy shift $\Delta_n(k)$ has the form

$$\begin{aligned} \Delta_n(k) &= \frac{1}{2} (\langle C_k | H_{\text{pert}} | C_k \rangle + \langle S_k | H_{\text{pert}} | S_k \rangle) \\ &= M \frac{1}{L} \sum_l \left(\frac{1}{R^2} - \kappa_l^2 \right) \cos \frac{2\pi k}{L} \end{aligned} \quad (\text{B13})$$

and the splitting energy $\delta_n(k)$ is given by

$$\begin{aligned} \delta_n(k) &= \langle C_k | H_{\text{pert}} | C_k \rangle - \langle S_k | H_{\text{pert}} | S_k \rangle \\ &= -M \frac{1}{L} \sum_l \cos \left(\frac{4\pi k}{L} \right) \kappa_l^2 \cos \frac{2\pi k}{L}. \end{aligned} \quad (\text{B14})$$

Inserting Eq. (B11) into Eq. (B13) we get that in the limit of weak charge-curvature coupling ($w \ll 1$) and smooth deformations ($m \ll 1$)

$$\Delta_n(k) \approx -M m^2 \frac{w^2}{8R^2} \cos \frac{2\pi k}{L}. \quad (\text{B15})$$

It is clear from Eq. (42) that for small m

$$m = 4\sqrt{2} \sqrt{\frac{4}{n^2} G\nu - 1} \quad (\text{B16})$$

and therefore

$$\Delta_n(k) \approx -M \frac{w^2}{4R^2} \left(\frac{4}{n^2} G\nu - 1 \right) \cos \frac{2\pi k}{L}. \quad (\text{B17})$$

Introducing Eq. (B11) into Eq. (B14), we see that in the zeroth-order perturbation theory the degeneracy of the exciton levels is removed for states with $2k=nj$, ($j=1, 2, \dots$). This means, in particular, that all exciton states (B9) of the elliptically deformed chain ($n=2$) split and the maximal splitting takes place for the state with $k=1$. In the limit of small w and m this splitting is given by

$$\delta_2(1) = M \frac{mw}{2R^2} \cos \frac{2\pi}{L}, \quad (\text{B18})$$

where m is given by Eq. (B16). $\delta_n(k)=0$ for $n=3, 5, \dots$. Thus in the order of our approximation all states of polygons with odd number of sides remain degenerate.

-
- [1] A. L. Kholodenko and T. A. Vilgis, Phys. Rep. **298**, 254 (1998).
[2] J. Wolfgang, S. M. Risser, S. Priyardshy, and D. N. Beratan, J. Phys. Chem. **101**, 2986 (1997).
[3] J. Feitelson and G. McLendon, Biochemistry **30**, 5051 (1991).
[4] D. Viduna, K. Hinsens, and G. Kneller, Phys. Rev. E **62**, 3986 (2000).
[5] P. O'Neil and E. M. Fielden, Adv. Radiat. Biol. **17**, 53 (1993).
[6] J. B. Retel, B. Hoebee, J. E. F. Braun, J. T. Lutgerink, E. van den Akker, A. H. Wanamarta, H. Joenje, and M. V. M. Lafleur, Mutat. Res. **299**, 165 (1993).
[7] E. A. Boon, A. L. Livingston, H. H. Chmiel, S. S. David, and J. K. Barton, Proc. Natl. Acad. Sci. U.S.A. **100**, 12543 (2003).
[8] K.-H. Yoo, D. H. Ha, J.-O. Lee, J. W. Park, Jinhee Kim, J. J. Kim, H.-Y. Lee, T. Kawai, and Han Yong Choi, Phys. Rev.

- Lett. **87**, 198102 (2001).
[9] S. S. Alexandre, E. Artacho, Jos M. Soler, and H. Chacham, Phys. Rev. Lett. **91**, 108105 (2003).
[10] E. M. Conwell and S. V. Rakhmanova, Proc. Natl. Acad. Sci. U.S.A. **97**, 4557 (2000).
[11] S. Komineas, G. Kalosakas, and A. R. Bishop, Phys. Rev. E **65**, 061905 (2002).
[12] G. Kalosakas, K. O. Rasmussen, and A. R. Bishop, J. Chem. Phys. **118**, 3731 (2003).
[13] J. L. Ting and M. Peyrard, Phys. Rev. E **53**, 1011 (1996); K. Forinash, T. Cretegny, and M. Peyrard, *ibid.* **55**, 4740 (1997).
[14] T. B. Polyakova and R. A. Suris, Solid State Commun. **77**, 825 (1991).
[15] Yu. B. Gaididei, S. F. Mingaleev, and P. L. Christiansen, Phys. Rev. E **62**, R53 (2000); P. L. Christiansen, Yu. B. Gaididei,

- and S. F. Mingaleev, *J. Phys.: Condens. Matter* **13**, 1181 (2001).
- [16] J. F. R. Archilla, P. L. Christiansen, S. F. Mingaleev, and Yu. B. Gaididei, *J. Phys. A* **34**, 6363 (2001); J. Cuevas, J. F. R. Archilla, Yu. B. Gaididei, and F. R. Romero, *Physica D* **163**, 106 (2002); J. F. R. Archilla, P. L. Christiansen, and Yu. B. Gaididei, *Phys. Rev. E* **65**, 016609 (2002).
- [17] R. Reigada, J. M. Sancho, M. Ibanes, and G. P. Tsironis, *J. Phys. A* **34**, 8465 (2001); M. Ibanes, J. M. Sancho, and G. P. Tsironis, *Phys. Rev. E* **65**, 041902 (2002).
- [18] S. F. Mingaleev, Yu. B. Gaididei, P. L. Christiansen, and Yu. S. Kivshar, *Europhys. Lett.* **59**, 403 (2002).
- [19] P. L. Hansen, D. Svensek, V. A. Parsegian, and R. Podgornik, *Phys. Rev. E* **60**, 1956 (1999).
- [20] T. E. Cloutier and J. Widom, *Mol. Cell* **14**, 355 (2004).
- [21] R. J. Cogdell, A. T. Gardiner, A. W. Roszak, C. J. Law, J. Southall, N. W. Isaacs, *Photosynthesis Research* **81**, 207 (2004).
- [22] G. McDermott, S. M. Prince, A. A. Freer, A. M. Hawthornthwaite-Lawless, M. Z. Papiz, R. G. Cogdell, N. W. Isaacs, *Nature (London)* **374**, 517 (1995).
- [23] M. Ketelaars, A. M. van Oijen, M. Matsushita, J. Köhler, J. Schmidt, and T. J. Aartsma, *Biophys. J.* **80**, 1591 (2001).
- [24] A. M. van Oijen, M. Ketelaars, J. Köhler, T. J. Aartsma, and J. Schmidt, *Science* **285**, 400 (1999).
- [25] M. Bopp, A. Sytnik, T. D. Howard, R. J. Cogdell, and R. M. Hochstrasser, *Proc. Natl. Acad. Sci. U.S.A.* **96**, 11271 (1999).
- [26] M. Matsushita, M. Ketelaars, A. M. van Oijen, J. Köhler, T. J. Aartsma, and J. Schmidt, *Biophys. J.* **80**, 1604 (2001).
- [27] X. Hong, Yu-X. Weng, and M. Li, *Biophys. J.* **86**, 1082 (2004).
- [28] S. Bahatyrova, R. N. Frese, K. O. van der Werf, C. Otto, C. N. Hunter and J. D. Olsen, *J. Biol. Chem.* **279**, 21327 (2004).
- [29] C. Dellago, M. M. Naor, and G. Hummer, *Phys. Rev. Lett.* **90**, 105902 (2003).
- [30] L. Onsager and M. Dupuis, *Rc. Sci. Int. Fis* **10**, 294 (1960).
- [31] C. V. Chaubal and L. G. Leal, *J. Polym. Sci., Part B: Polym. Phys.* **37**, 281 (1999).
- [32] F. B. Beleznyay *et al.*, *J. Chem. Phys.* **124**, 074708 (2006).
- [33] Note that our approach is also valid for the case when carriers are long-lived excitons (e.g., triplet excitons). The exciton-curvature interaction [an analog of Eq. (2)] stems from the so-called $D_{nn'}$ term in the theory of molecular excitons. It is defined as a change in the interaction energy between subunits n and n' in the transition of one of them to the excited state [see A. S. Davydov, *Theory of Molecular Excitons* (Plenum, New York, 1971)].
- [34] M. Abramowitz and I. Stegun, *Handbook of Mathematical Functions* (Dover Publications, New York, 1972).
- [35] M. Doi and S. F. Edwards, *The Theory of Polymer Dynamics* (Clarendon Press, Oxford 1986).
- [36] A. F. Jalbout, K. Y. Pichugin, and L. Adamowicz, *Eur. Phys. J. D* **26**, 197 (2003).
- [37] J. G. Gay and B. J. Berne, *J. Chem. Phys.* **74**, 3316 (1981).
- [38] R. J. Pugh *et al.*, *Biochim. Biophys. Acta* **1366**, 301 (1998).
- [39] D. Fotiadis *et al.*, *J. Biol. Chem.* **279**, 2063 (2004).
- [40] Yu. Gaididei, N. Flytzanis, and O. Yanovitskii, *Phys. Lett. A* **185**, 401 (1994).
- [41] R. Mittal and I. A. Howard, *Phys. Rev. B* **53**, 14 171 (1996).
- [42] I. A. Howard and R. Mittal, *Phys. Rev. B* **57**, 45 (1998).